Revisiting Metal Sulfide Semiconductors: A Solution-Based General Protocol for Thin Film Formation, Hall Effect Measurement, and Application Prospects

Dipak V. Shinde, Supriya A. Patil, Keumnam Cho, Do Young Ahn, Nabeen K. Shrestha, Rajaram S. Mane, Joong Kee Lee, and Sung-Hwan Han**

Nanostructured thin films of metal sulfides (MS) are highly desirable materials for various optoelectronic device applications. However, a general low-temperature protocol that describes deposition of varieties of MS structures, especially in their film form is still not available in literatures. Here, a simple and highly effective general solution-based deposition protocol for highly crystalline and well-defined nanostructured MS thin films from ethanol on variety of conducting and non-conducting substrates is presented. The films display remarkable electronic properties such as high carrier mobility and high conductivity. When NiS thin film deposited on a flexible polyethylene terephthalate (PET) substrate is used as a fluorine doped tin oxide (FTO)-free counter electrode in dye-sensitized solar cells, it exhibits a solar-to-electric power conversion efficiency of 9.27 ± 0.26% with the highest conversion efficiency as high as 9.50% (vs 8.97 ± 0.07% exhibited by Pt-electrode). In addition, the NiS film deposited on a Ti-foil has demonstrated an outstanding catalytic activity for the hydrogen and oxygen evolution reactions from water.

1. Introduction

Metal sulfides (MS) are interesting class of materials having distinct optoelectronic properties that have scientific as well as technological importance. A wide variety of devices such as solar cells, supercapacitors, photodetectors, lithium ion batteries, transistors, light-emitting diodes, water splitting catalysts, fuel cell catalysts, etc., employ nanostructured MS.[1–8] For utilization of MS films in these devices, a general solution-based deposition method, which is facile, benign, and which can deposit a uniform MS thin films is highly desirable. Although various available techniques such as chemical vapor deposition,[9,10] atomic layer deposition,[11,12] molecular beam epitaxy,[13,14] electrodeposition,[7,15] successive ionic layer adsorption and reaction,[16,17] vapor sublimation,[18] etc., are able to produce thin films of MS, they lack generality or need sophisticated instrumentation, and are complicated. In this context, chemical bath deposition is inarguably the simplest method for thin film deposition. Generally, a suitable complexing agent and pH regulating agents are added in order to avoid spontaneous precipitation in an aqueous bath, which makes the process complicated due to extremely critical optimization for concentration of complexing agents and pH adjustment for an individual MS case.[4,19–22] As a result, development of MS films by solution-based method has often been a case of trial-and-error with poor reproducibility, which remained as an unexplored research field yet in material science and technology. In order to tackle the above problems in aqueous solution, the film deposition reaction is carried out in ethanol solution without the use of any complexing and/or pH-regulating agents. This protocol relies on dissolution of metal salts and thioacetamide in ethanol and heating the solutions at 70 °C. Although very few reports on MS film deposition from nonaqueous solution has been reported,[23,24] no general protocol is available that can be applied overall to deposit all variety of MS thin films under similar conditions with good reproducibility. The proposed protocol is extremely simple and general, which can lay simple guidelines to fabricate almost all types of metal sulfides uniformly over all area of the substrate, provided that the corresponding metal salts are soluble in ethanol. The as-deposited MS films are highly crystalline even without thermal treatment. Interestingly, the films can be directly grown on variety of conducting as well as non-conducting substrates such as glass, plastic, fluorine doped tin oxide (FTO), Ti-foil, carbon paper, Whatman filter paper, etc., which can be of great technological importance. As an example of potential application of these thin films, we demonstrate the use of NiS film deposited on flexible plastic substrates as FTO-free dual-functioned (electronic support + electrocatalytic) counter electrode in dye-sensitized solar cells

Dr. D. V. Shinde,[+] S. A. Patil, K. Cho, D. Y. Ahn, Dr. N. K. Shrestha, Prof. S.-H. Han
Department of Chemistry
Hanyang University
Seoul 133-791, Republic of Korea
E-mail: nabeenkshrestha@hotmail.com; shhan@hanyang.ac.kr

Prof. R. S. Mane
School of Physical Sciences
Swami Ramanand Teerth Marathwada University
Nanded-431 606, India

Prof. J. K. Lee
Energy Storage Research Center
Korea Institute of Science and Technology
Seoul 136-791, Republic of Korea

[+]Present address:Department of Chemical Engineering, Pohang University of Science & Technology, Pohang, Gyeonbuk 790-784, Republic of Korea.

DOI: 10.1002/adfm.201500964

(DSSCs), which has exhibited the superior catalytic activity towards triiodide reduction, showing better photovoltaic performance as compared to the universally accepted benchmark counter electrode consisting of Pt-film on a FTO substrate. In addition, study demonstrates that NiS film deposited on a Ti-substrate can be a very promising electrocatayst for water splitting.

2. Results and Discussion

Optical images and the corresponding morphology of various MS films deposited onto non-conducting glass substrate from the ethanolic bath are presented in Figure S1 (Supporting Information) and **Figure 1**, respectively. In all cases, the films were highly uniform and had great surface coverage over the entire substrate. It is noteworthy that the formation of MS film following this protocol shows quite excellent reproducibility over all metal elements. Due to difference in relative affinity of metal ions towards sulfide ions, the rate of each reaction was found to be different. For example, Sn^{2+} and Bi^{3+} ions reacted very quickly with thioacetamide to form SnS_2 and Bi_2S_3 respectively, while the reactions of Co^{+2} and Ag^{+} were sluggish. As a result of different deposition kinetics, each sulfide film of different metal has different microstructures in Figure 1. In order to understand the mechanism behind the reactions that can be successfully carried out for the deposition of MS without the use of any complexing agent, we analyzed the relative polarity difference between water (dielectric constant = 80.4) and ethanol (dielectric constant = 24.3). Owing to the low polarity of ethanol, we noticed the metal salts (e.g., $SnCl_4$, $SnCl_2$, $BiCl_3$) that can be easily hydrolyzed in water producing metal hydroxides are reasonably stable. In addition, the metal salts, which react faster with thioacetamide to precipitate MS spontaneously in water, react languidly in ethanol. We assume that the deposition of MS thin film occurs by complex formation mechanism, the details of which are explained in Figure S2 (Supporting Information). X-ray diffraction (XRD) patterns of various MS films are shown in **Figure 2** and Figure S3 (Supporting Information), which reveal that even without post annealing, the as-deposited films by the proposed protocol are highly crystalline. Utilization of volatile and non-polar ethanol solvent suppress incorporation of OH^{-} species into MS thin film by increasing their crystallinities with slow reaction time, which can find wide applications in optoelectronics, especially for low temperature processes.

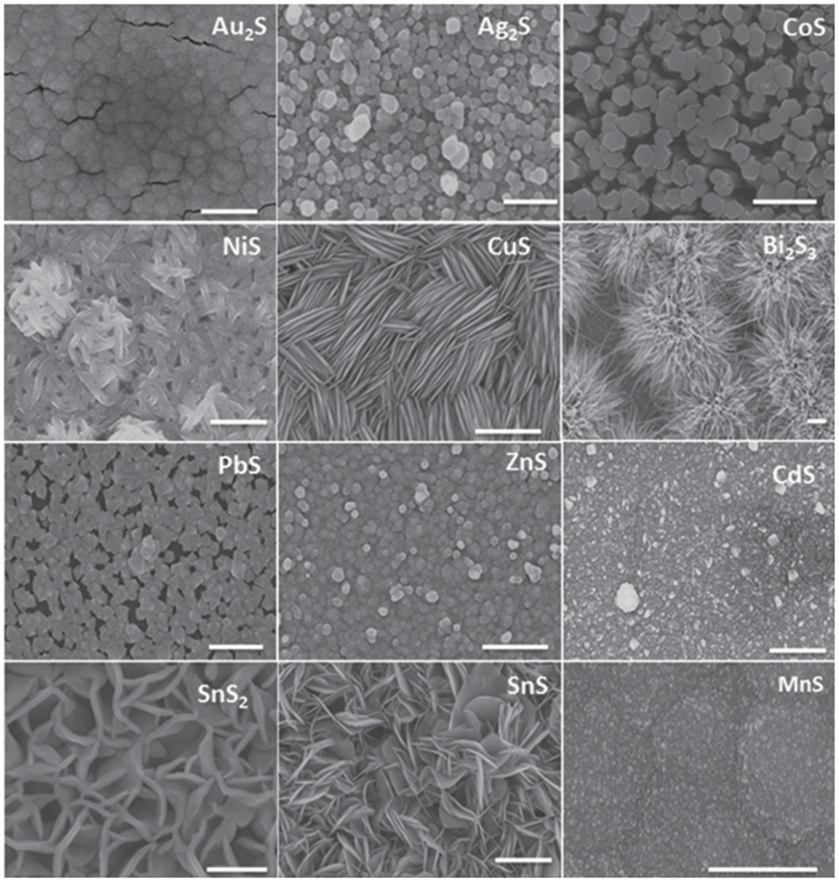

Figure 1. Scanning electron microscopy images (false colored) of various metal-sulfides on glass substrates. The scale bar in each image corresponds to 500 nm.

It is worthy to note that there are very limited literatures on electronic properties such as carrier concentration, mobility, and conductivity of various MS films.[25–34] Moreover, there has been no systematic database on the same, and the available literature database on the above electronic properties can be found only for MS films, which were deposited by different methods especially at high temperatures (**Table 1**). As these electronic properties depend on the film quality as well on the method of measurement, it would not be reliable to compare the quantitative data of the electronic properties of individual MS films prepared and measured by different methods. Therefore, study on the above electronic properties of the MS films having similar film quality prepared by a single method is highly desirable and significantly important for future applications. In the present study, quantitative data on the electronic properties of all MS films synthesized by the proposed protocol has been evaluated using Hall effect measurements, and a systematic data base of the MS films describing their carrier concentration, carrier mobility, and conductivity, which are very important for thin film technology has been established together with the available earlier reports (Table 1). We believe that such a simple and general protocol to deposit large variety of MS particularly in thin film form along with their database on electronic properties provides very useful and fundamental information for physicists and material scientists working on thin film semiconductor devices. However, it should be worthwhile to note that the MS films of the reported data were synthesized differently in each case. Therefore, it is not reliable to compare the conductivity and charge carrier mobility of the MS films deposited by the proposed protocol to those reported

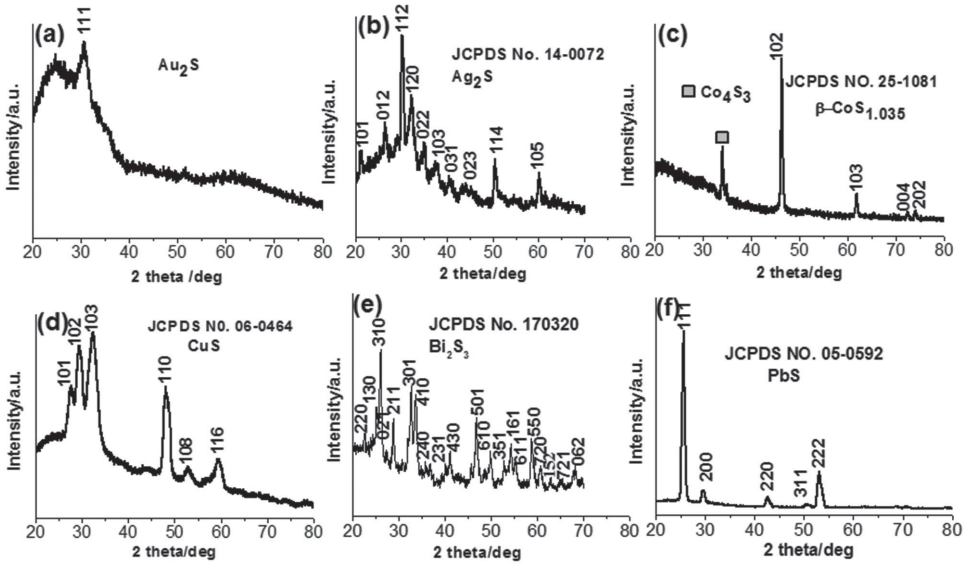

Figure 2. XRD patterns of various MS thin films.

Table 1. Conductivity, charge carrier concentration, and mobility of various MS films deposited by the proposed protocol) obtained by Hall effect measurements at 25 °C.

Metal sulfide	Conductivity [S cm^{-1}]	Carrier conc. [cm^{-3}]	Mobility [cm^2 V^{-1} s^{-1}]	Carrier type	Remarks
Au_2S	1.16×10^{-4}	6.12×10^{12}	324	P	This work
–	–	–	–		
Ag_2S	1.29×10^{-4}	-8.26×10^{13}	9.70	N	This work
–					
Co_4S_3	9.50×10^{2}	4.72×10^{22}	0.12	P	This work
–	–	–	–		
NiS	1.80×10^{3}	-3.46×10^{22}	0.32	N	This work
$^{R}Ni_{1-x}S$	3.10×10^{2}	-3.30×10^{20}	6.00		Depositedat 727 °C on SiO_2.[25]
CuS	3.00×10^{3}	1.18×10^{22}	1.58	P	This work
^{R}CuS	2.00×10^{2}	1.00×10^{20}	2.00		ALD/air exposure[26]
Bi_2S_3	1.09×10^{-4}	3.32×10^{14}	2.05	P	This work
$^{R}Bi_2S_3$	–	5.53×10^{16}	210.3		Hydrothermal, 200 °C/pressed F film[27]
PbS	3.70×10^{-4}	4.56×10^{13}	50.8	P	This work
^{R}PbS	–	9.00×10^{7}	278		CBD[28]
ZnS	3.25×10^{-4}	-5.69×10^{14}	3.57	N	This work
^{R}ZnS	9.32×10^{-4}	-4.88×10^{14}	11.9		Thermal evaporation[29]
CdS	3.50×10^{-5}	-5.51×10^{14}	0.39	N	This work
^{R}CdS	3.30×10^{-4}	-9.70×10^{14}	2.1		CBD[30]
SnS_2	1.17×10^{-4}	-6.27×10^{13}	11.6	N	This work
$^{R}SnS_2$	1.30×10^{-1}	$-5.\ 20 \times 10^{16}$	18.3		Single crystal/CBD at 450 °C[31]
SnS	3.40×10^{-5}	1.13×10^{12}	18.9	P	This work
^{R}SnS	1.70×10^{-2}	6.90×10^{15}	15.3		ALD/200 °C[32]
MnS	3.70×10^{-4}	4.56×10^{13}	50.8	P	This work
^{R}MnS	4.30×10^{-6}	–	80		CBD on glass[33]

^{R}denotes the previously reported data.

previously for the corresponding compounds. To the best of our knowledge, gold sulfide in film state is reported here for the first time. This film has exhibited the highest carrier mobility of 324 $cm^2\ V^{-1}\ s^{-1}$, which shows its potential application in high speed electronic devices. The NiS film exhibited a rather lower carrier mobility of 0.32 $cm^2\ V^{-1}\ s^{-1}$, but high carrier concentration of $3.46 \times 10^{22}\ cm^{-3}$ and high conductivity of 1800 S cm^{-1}. The high conductivity of the NiS films is attributed to strongly hybridized Ni 3d and S 3p orbitals.[35] Similarly, CuS films also shows high carrier concentration of $1.18 \times 10^{22}\ cm^{-3}$ and high conductivity of 3000 S cm^{-1}. Thin films of MnS, SnS, and PbS showed remarkable charge carrier mobilities of 50.8, 18.9, and 50.8 $cm^2\ V^{-1}\ s^{-1}$, respectively. To see the reproducibility of the film formation and the variance on their electronic properties, five replicas of the NiS film were produced and their electronic properties were characterized using Hall effect measurement. Table S2 (Supporting Information) shows that out of five, four samples exhibit the electronic properties very close to those shown in Table 1, whereas one sample shows little deviated electronic properties but the deviation is still within the acceptable range. This finding supports the reproducibility of the proposed protocol for MS film formation with the electronic properties very close to those shown in Table 1. Very interestingly, some of the p-type MS films in Table 1 show higher conductivity and carrier mobility than organic hole transporting materials used in solid-state photovoltaic devices.[36–40] Therefore, these MS films could be used as a highly efficient inorganic hole transporting materials in optoelectronic devices,[38] which could enhance the stability of the devices compared to the devices based on organic hole transporting materials.

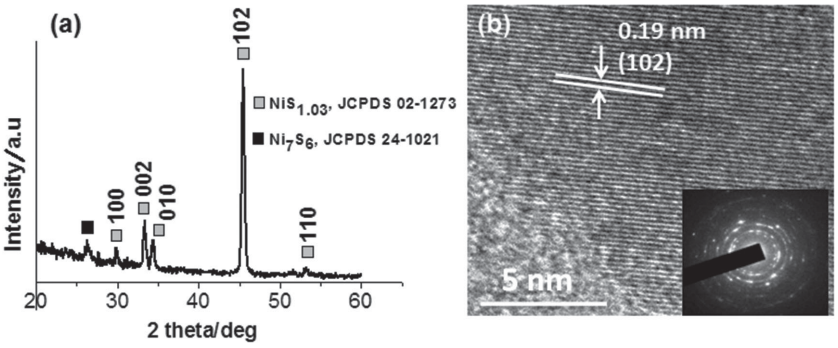

Figure 3. a) XRD pattern of NiS film deposited on glass substrate. b) High-resolution transmission electron microscope image of NiS showing the lattice spacing of 0.19 nm corresponding to the (102) plane. Inset of the figure shows selected area electron diffraction patterns of NiS.

Apart from the application of MS in electronic and optoelectronic devices, they have also been demonstrated recently as potential candidates for electrocatalytic electrode materials in DSSCs.[7,8,35] To date, Pt-coated FTO electrode has demonstrated the so far champion performance,[41] and hence it has been universally accepted benchmark for the DSSC counter electrode. However, due to very high price of Pt, recently materials such metal chalcogenides, metal oxides, metal nitrides, various composites, carbon, and polymer materials, obtained especially from high temperature and tedious process have been suggested in the literature as alternative materials for Pt counter electrode.[7,8,35,42–56] Among MS counter electrodes prepared by various methods,[7,8,35,42–56] NiS electrode prepared by deposition of NiS film on a nickel foam, by solvothermally reacting the foam with elemental sulfur in ethanol, has demonstrated the best performance of the DSSC with power conversion efficiency of 8.55%.[42] This value is smaller nearly by 1% to those of the $Co_{0.85}Se$ (E_{ff} = 9.40%) and reduced graphene (E_{ff} = 9.54%).[57,58] To the best of our knowledge, these are the best two Pt-free counter electrodes showing the highest power conversion efficiency.[49,57,58] Based on the reports of metal chalcogenide counter electrodes, it is worthy to investigate the electrocatalytic activity of the NiS as a model MS film for DSSC counter electrode prepared by the proposed protocol. In the following, we discuss the complete characterization and the electrocatalytic activities of NiS film towards triiodide reduction in DSSCs. The XRD pattern of the NiS film deposited on a glass substrate shows high crystallinity with the (102) dominant plane (**Figure 3**a). The film exhibited $NiS_{1.03}$ as an abundant phase with some impurity from Ni_7S_6 phase. The crystal structure is further investigated using high-resolution transmission electron microscope (HR-TEM), which shows the (102) plane lattice spacing of 0.19 nm (Figure 3b). These data are well in line with the XRD data of Figure 3a. In addition, the selected area electron diffraction (SAED) pattern in the inset of Figure 3b shows crystalline nature of the film, which is also in good agreement with the XRD pattern shown in Figure 3a. The chemical composition of the NiS film was determined using X-ray photoelectron spectroscopy (XPS), which confirms the nickel monosulfide species (Figure S4, Supporting Information). It should be noted that the XPS depth profile of an aged NiS film reveals that the material is quite stable against atmospheric oxidation even when the film was stored for a long time at room temperature and pressure in dark (Figure S5, Supporting Information). In addition, the NiS films grown on various non-conducting substrates (Figure S6, Supporting Information) have demonstrated better conductivity than that of FTO- and ITO-coated glass substrate (Figure S7, Supporting Information).

In contrast to various Pt-free counter electrode materials fabricated especially at high temperature and tedious process,[48] we demonstrate here that the NiS film deposited on flexible polyethyelne terephthalate (PET) plastic substrate using the proposed low temperature protocol shows it as a FTO-free counter electrode of DSSCs with a better performance than that of the benchmark Pt-coated FTO electrode. Inset picture in **Figure 4**a shows the optical image of NiS deposited on a PET substrate. The film on PET substrates was very mechanically robust, and did not show visual cracks or detachment from the surface upon bending. Figure 4a shows the cyclic voltammograms (CVs) of NiS and Pt film counter electrodes in acetonitrile containing iodine/iodide redox couple. Two redox peaks observed in each CV are due to the reversible $I_3^- + 2e^- \leftrightarrow 3I^-$, and $2I_3^- \leftrightarrow 3I_2 + 2e^-$ redox reactions. Catalytic activity of the electrode in DSSCs is related to the first redox reaction occurring at more negative potential in CV,[7] where both the electrodes have exhibited the similar peak separation, indicating the competitive catalytic

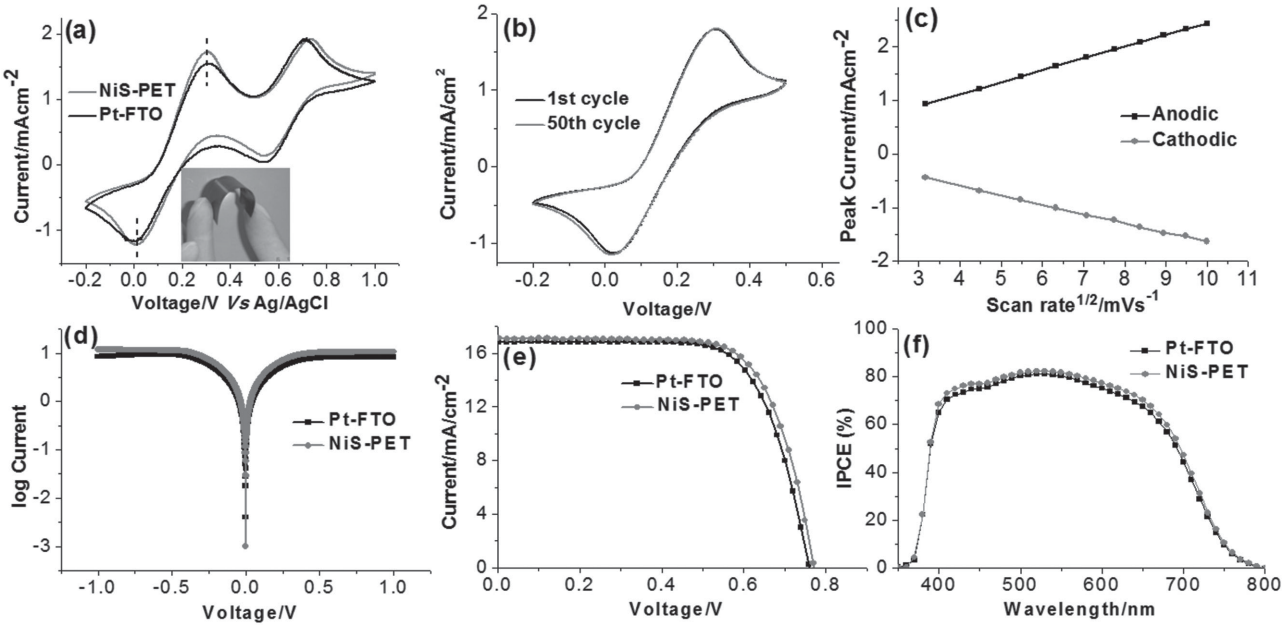

Figure 4. a) Cyclic voltammograms of the Pt and NiS electrodes in an acetonitrile containing 0.1 M $LiClO_4 + 5 \times 10^{-3}$ M $I_2 + 10 \times 10^{-3}$ M LiI at a sweep rate of 50 mV s^{-1}. Inset shows the photograph of flexible NiS electrode. b) Stability test of flexible NiS electrode. c) A plot of square root of scan rate vs anodic and cathodic peak current obtained from CV measurements of NiS electrodes. d) Tafel polarization curves of the symmetrical cells fabricated using two identical counter electrodes with the cell structure-counter electrode/electrolyte/counter electrode. e) Current–voltage plots of DSSCs obtained using Pt and flexible NiS counter electrodes under simulated emission of 1 sun radiation. f) Photocurrent action spectra (IPCE) curves of DSSCs employing Pt and flexible NiS as counter electrodes.

activity. However, it should be noted that the NiS electrode has exhibited quantitatively a little higher current density than that of the Pt. This indicates that the NiS electrode can catalyze the triiodide reduction more effectively in DSSCs. We further studied the electrochemical stability of the NiS for 50 catalytic cycles in the range of –0.2 to 0.5 V (Figure 4b), which reveals that the electrode is quite stable in the electrolyte with no sign of degradation. The observed linear plots in Figure 4c reveal that triiodide reduction on NiS is surface catalytic reaction and is a diffusion limited process. To further compare the electrocatalytic activity of the NiS and Pt electrodes, Tafel polarization curves were measured using the symmetrical cells fabricated using two identical counter electrodes and the same electrolyte as used in DSSCs. Apparently, the NiS–PET electrode shows higher exchange current density (Figure 4d), indicating its higher catalytic activity towards triiodide reduction. The current–voltage (*J*–*V*) plots of DSSCs fabricated using the NiS–PET and Pt–FTO electrodes are shown in Figure 4e, and the detailed photovoltaic parameters are summarized in Figure S8 and Table S3 (Supporting Information). The NiS counter electrode-based DSSC of the present work shows the closer but even little better power conversion efficiency of 9.27 ± 0.26% with the highest conversion efficiency as high as 9.50% as compared to the power conversion efficiency of 8.97 ± 0.07% demonstrated by the Pt–FTO counter electrode-based DSSC. The overall better photovoltaic performance of the DSSCs utilizing the NiS counter electrode is also supported by the incident photon-to-current conversion efficiency (IPCE) spectra shown in Figure 4f. It is important to note that the counter electrode prepared by the proposed protocol has demonstrated a better performance of the device as compared to the early reported best counter electrode of NiS deposited on nickel foam.[42] The power conversion efficiency demonstrated by the NiS–PET counter electrode-based device is closer to those of the $Co_{0.85}Se$ and reduced graphene—the best two counter electrodes reported for DSSCs.[57,58] Moreover, the present work has used the NiS deposited on a flexible non-conducting plastic (PET) substrate as counter electrode, which further highlights the significance of the present work.

In a further experiment, NiS films were deposited on Ti-substrates (NiS–Ti), and the films were characterized with scanning electron microscope (SEM) (**Figure 5**a) and XRD (Figure 5b).

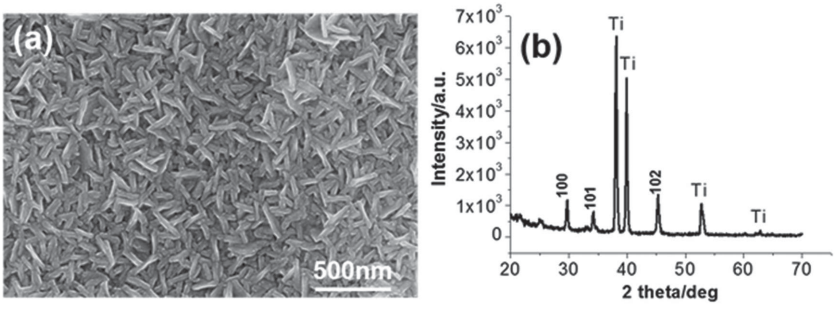

Figure 5. a) SEM image of NiS deposited on Ti foil substrate and b) XRD patterns of the same NiS film.

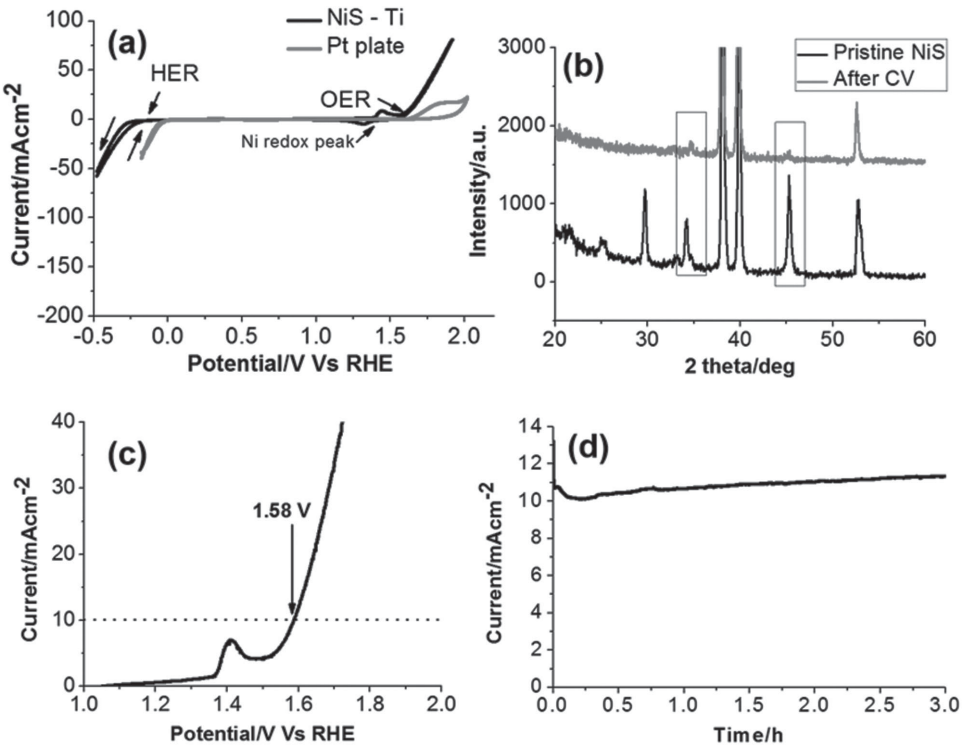

Figure 6. a) Cyclic voltammograms of NiS–Ti and Pt plate electrodes of area 1 cm^2 measured at a sweep rate of 5 mV s^{-1} in 1 M KOH electrolyte. b) XRD patterns of NiS film deposited on Ti substrate before and after 10 CV scans. c) Linear sweep voltammogram exhibited by NiS film deposited on Ti substrate in an aqueous solution of 1 M KOH at sweeping rate of 1 mV s^{-1}. Counter electrode was a Pt plate. d) OER current transient of the NiS–Ti electrode obtained by applying a constant potential of 1.6 V vs RHE.

The NiS–Ti electrode was investigated as an electrocatalyst for water splitting reactions. **Figure 6**a shows CVs of the NiS–Ti electrode and Pt plate electrodes in 1 M KOH aqueous solution. An oxidation wave appeared at approximately 1.44 V suggests the conversion of NiS to OER active γ-NiOOH phase in the first scan to the anodic potentials.[59] The XRD pattern of the NiS electrode obtained after voltammetry measurement shows a decrease in peak intensities of the NiS phase as compared to the pristine NiS (Figure 6b). Meanwhile, no peaks corresponding to $Ni(OH)_2$ or γ-NiOOH can be observed in Figure 6b, which indicates their amorphous nature.[59] After an oxidation peak of Ni (+2 to +3),[59] a sharp rise in current at a potential of 1.55 V with an onset potential of 1.50 V (overpotential of ≈0.27 V) for oxygen evolution reaction (OER) can be noticed in the anodic scan. When a linear sweep voltammetry in anodic direction was performed, it achieved 10 mA cm^{-2} of OER current density (a metric relevant to solar fuel synthesis) at a moderate over potential of 0.35 V (Figure 6c).

It is worthwhile to note that this catalytic performance for OER favorably competes with some reported best OER catalysts. For example, a nitrogen-doped reduced graphene oxide–Co_3O_4 composite showed an onset potential of 1.50 V,[60] which is closer to that exhibited by RuO_2 catalyst (i.e., 1.48 V[61]. Meanwhile the hydrothermally synthesized $Ni(OH)_2$ hollow sphere electrode showed an OER onset potential of 1.54 V, and OER current density of 10 mA cm^{-2} at an overpotential of 0.33 V,[59] which is closer to the overpotential of 0.36 V[61] exhibited by RuO_2 catalyst. When a constant potential of 1.60 V was applied to the NiS electrode, and the OER current was monitored over a period of 3 h, the electrode demonstrated a highly stable catalytic performance as shown by the current transient curve in Figure 6d. On the other hand, the CVs in Figure 6a also shows the hydrogen evolution reaction (HER) from 1 M KOH solution at the overpotential of ≈0.22 V in cathodic scan. This finding suggests that NiS–Ti electrodes have electrocatalytic property for overall splitting of water. However, the above overpotential for HER in Figure 6a is larger than that exhibited by the Pt-free electrodes such as MoS_2 and WS_2–RGo composite electrodes, which have demonstrated an excellent HER activity in acidic medium.[62–65] Hence, we further investigated the catalytic activity of the NiS–Ti electrode towards HER in 0.5 M H_2SO_4 solution, which demonstrated the evolution of hydrogen at a small overpotential of 0.12 V (**Figure 7**a). This activity is comparatively better than that demonstrated previously by the MoS_2 and WS_2–RGo composite electrodes. For example, MoS_2 catalysts have an overpotential ranging from 0.20 to 0.15 V.[62–64] Similarly, a WS_2–RGo composite catalyst synthesized by hydrothermal method showed an overpotential of 0.15 V[65] for HER, which is even little larger than the overpotential of 0.12 V exhibited by the NiS–Ti electrode. In addition, it is important to mention that most of the catalysts reported in the literature have complex and difficult synthetic procedures compared to the proposed general protocol of the present work. We further investigated the stability of the electrode in acidic medium by chronoamperometry. Figure 7b shows the current transient curve at an applied potential of 0.13 V over the course

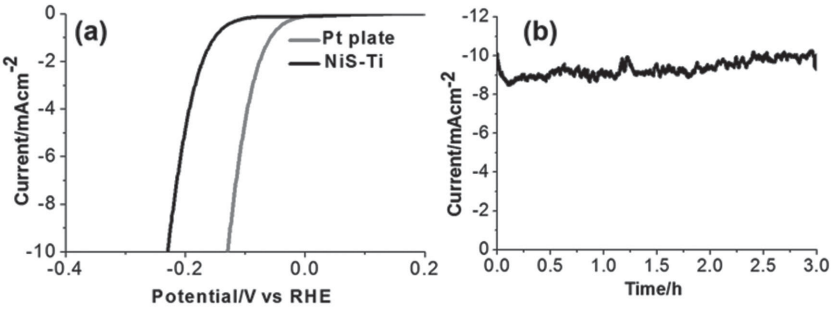

Figure 7. a) Linear sweep voltammogram of NiS–Ti and Pt electrodes in 0.5 M H_2SO_4 solution measured at a sweep rate of 1 mV s^{-1}. b) HER current transient of the NiS–Ti electrode obtained by applying a constant potential of 0.13 V vs RHE.

of 3 h continuous electrolysis. The slight fluctuations of current observed in the transient curve are due to vigorous evolution of hydrogen bubbles and their subsequent detachment from the electrode surface. However, the current transient curve clearly demonstrates that the NiS film is quite stable at this operating condition with no sign of degradation. Further detail studies of various MS thin films on water splitting are undergoing.

3. Conclusion

In summary, we have developed a novel, low-temperature, and general solution-based protocol, which works equally for deposition of most of the MS nanostructured thin films. The films obtained by this protocol were crystalline and highly uniform. The films can be deposited on any desirable conductive as well as non-conductive substrates. MS films fabricated using this protocol exhibited many interesting comparative/superior properties such as high conductivities and high charge carrier mobilities. Considering the fact that variety of devices such as solar cells, photodetectors, transistors, supercapacitors, electrocatalysts, etc., require the crystalline material in thin film form, the current protocol provides an easy and low-cost approach for deposition of these films with high reproducibility. The NiS film deposited on a flexible PET substrate demonstrated as a highly potential material for the current collector and electrocatalyst. As compared to the benchmark Pt–FTO electrode, the NiS–PET electrode exhibited superior electrocatalytic activity towards triiodide reduction in DSSCs leading to the solar-to-electric power conversion efficiency of 9.27 ± 0.26% with the highest conversion efficiency as high as 9.50% (against 8.97 ± 0.07% exhibited by the Pt–FTO electrode). On the other hand, in another experiment, NiS film deposited on a Ti-substrate showed a very promising electrocatalyst for water splitting reactions. Thus, this work demonstrates that MS films deposited using the proposed protocol could be a promising candidate for substitution of Pt and other precious metals used in electrocatalysis.

4. Experimental Section

Deposition of MS Films: All the reagents used in this experiment were of analytical grade and obtained from Sigma Aldrich, Korea. All the metal-sulfide (MS) films were deposited by the same protocol from ethanolic solutions. The deposition conditions for various MS films are shown in Table S1 (Supporting Information). In general, equimolar (0.1 M) metal salts and thioacetamide were dissolved in ethanol (≥99.5%) in falcon tubes of 50 mL capacity. For the deposition of lead sulfide (PbS), the metal salt (i.e., $PbCl_2$) concentration is taken as 0.01 M as it is partially soluble in ethanol. In the case of SnS_2, excess (optimized as three times to that of metal salts) sulfur source (i.e., thioacetamide) is required. Some MS films were found to be peeled off for a prolong deposition (longer than 10 h). In these cases, the deposition was terminated after 6 h. (Table S1, Supporting Information). The films were deposited onto various substrates having the area of 2.5 × 7.5 cm^2. For the deposition, cleaned substrates were dipped in the solutions followed by closing the lids of the falcon tubes tightly and performing the reaction in a water bath at 70 °C for a desired time. After the deposition, the films were washed with ethanol, dried in stream of argon, and stored under dark before characterizations. NiS films deposited on the flexible PET substrates were used as counter electrodes in DSSCs. Photoanodes of TiO_2 were prepared by doctor blade technique as described elsewhere.[1] The TiO_2 films were sensitized with N719 dye by immersing in the dye solution (0.5×10^{-3} M in 1:1 acetonitrile: ethanol solvent mixture) for 24 h. The sensitized films were washed with ethanol, dried, and kept in dark.

Characterizations: Phase and crystal structures of all MS films were determined using a X-ray diffractometer (Rigaku D/MAX 2500 V, Cu Kα, λ = 0.15418 nm), a HRTEM (JEOL-2100F) and SAED analyzer. The morphology of the MS architectures deposited onto soda lime glass substrates was monitored using a field emission scanning electron microscope (FE-SEM, Hitachi S-4200). Chemical composition of NiS films were measured using a XPS (Thermo Fisher Scientific Co.) with twin Mg Kα source at a chamber base pressure of ≈10^{-10} Torr. Hall measurements of all the films deposited on glass substrates were performed using Van der Pauw method with Ecopia HMS-3000 Hall measurement system. For the measurement, the samples were cut into 1 × 1 cm^2 area and electrical contacts were made using soldering technique. Electrochemical water splitting activity of NiS films was investigated in a three-electrode electrochemical cell using NiS on a Ti-foil as working, Ag/AgCl (3 M NaCl) as reference and Pt plate as counter electrode. Active area of the samples was kept 1 cm^2. Aqueous solutions of 1 M KOH were used as electrolytes. Before measurements, the electrolytes were purged with Ar gas for 10 min. All the potentials measured against Ag/AgCl reference were converted to reversible hydrogen electrode (RHE) scale. The DSSC devices were assembled by scratching out the area of TiO_2 photoanodes to 0.25 cm^2. In order to measure the solar-to-electric power conversion efficiency, dye-loaded TiO_2 photoanodes on FTO were incorporated into a thin layer sandwich-type cells with a Pt-coated FTO (obtained by sputtering) or NiS films on PET foil as the counter electrode. A 50 μm thick polyimide film was used as a spacer between the photoanode and counter electrode and an Iodolyte AN-50 electrolyte (iodide-based low viscosity electrolyte with 50×10^{-3} M of triiodide in acetonitrile) was injected into the space. Cell performance was measured by irradiating with 100 mW cm^{-2} white light (1 sun) using a solar simulator (PEC-L01, Peccell), and the photocurrent was measured using a Keithley 2400 Source Meter. The IPCE was recorded without bias under illumination with respect to a calibrated Melles-Friot silicon diode and measured by changing the excitation wavelength (photon counting spectrometer, ISS Inc. and Keithley 2400). Impedance spectra of the symmetrical cells (i.e., Pt–Pt, NiS–NiS) were measured by sandwiching two identical counter electrodes with a 50 μm thick polyimide film as a spacer and injecting the electrolyte in between. Catalytic activity of the counter electrode was measured using cyclic-voltammetry technique in a three-electrode cell containing Pt–FTO (or NiS–PET) as working, Pt plate as counter, and Ag/AgCl (3 M NaCl) as

reference electrodes. The electrolyte used consisted of 5×10^{-3} M I_2, 10×10^{-3} M LiI, and 0.1×10^{-3} M $LiClO_4$ in acetonitrile.

Supporting Information

Supporting Information is available from the Wiley Online Library or from the author.

Acknowledgements

This research was supported by the KIST Institutional Program (2E23964) and by Basic Science Research Program through the National Research Foundation of Korea (NRF) funded by the Ministry of Education (2013009768).

Received: March 11, 2015
Revised: July 9, 2015
Published online: August 14, 2015

[1] M. Kokotov, G. Hodes, *Chem. Mater.* **2010**, *22*, 5483.
[2] M. R. Esmaeili-Rad, S. Salahuddin, *Sci. Rep.* **2013**, *3*, 2345.
[3] A. H. Ip, S. M. Thon, S. Hoogland, O. Voznyy, D. Zhitomirsky, R. Debnath, L. Levina, L. R. Rollny, G. H. Carey, A. Fischer, K. W. Kemp, I. J. Kramer, Z. Ning, A. J. Labelle, K. W. Chou, A. Amassian, E. H. Sargent, *Nat. Nanotechnol.* **2012**, *7*, 577.
[4] G. Hodes, *Chemical Solution Deposition of Semiconductor Films*, Marcel Dekker Inc., New York **2003**.
[5] Y. Du, Z. Yin, J. Zhu, X. Huang, X.-J. Wu, Z. Zeng, Q. Yan, H. Zhang, *Nat. Commun.* **2012**, *3*, 1177.
[6] L. Kranz, C. Gretener, J. Perrenoud, R. Schmitt, F. Pianezzi, F. La Mattina, P. Blösch, E. Cheah, A. Chirilă, C. M. Fella, H. Hagendorfer, T. Jäger, S. Nishiwaki, A. R. Uhl, S. Buecheler, A. N. Tiwari, *Nat. Commun.* **2013**, *4*, 2306.
[7] H. Sun, D. Qin, S. Huang, X. Guo, D. Li, Y. Luo, Q. Meng, *Energy Environ. Sci.* **2011**, *4*, 2630.
[8] C.-W. Kung, H.-W. Chen, C.-Y. Lin, K.-C. Huang, R. Vittal, K.-C. Ho, *ACS Nano* **2012**, *6*, 7016.
[9] N. Berry, M. Cheng, C. L. Perkins, M. Limpinsel, J. C. Hemminger, M. Law, *Adv. Energy Mater.* **2012**, *2*, 1124.
[10] A. N. MacInnes, M. B. Power, A. R. Barron, *Chem. Mater.* **1992**, *4*, 11.
[11] N. Naghavi, S. Spiering, M. Powalla, B. Cavana, D. Lincot, *Prog. Photovoltaics* **2003**, *11*, 437.
[12] J. R. Bakke, H. J. Jung, T. Tanskanen, R. Sonclair, S. F. Bent, *Chem. Mater.* **2010**, *22*, 4669.
[13] P. Boieriu, R. Sporken, Y. Xin, N. D. Browning, S. Sivananthan, *J. Electron. Mater.* **2000**, *29*, 718.
[14] W. Wang, K. K. Leung, W. K. Fong, S. F. Wang, Y. Y. Hui, S. P. Lau, Z. Chen, L. J. Shi, C. B. Cao, C. J. Surya, *Appl. Phys.* **2012**, *111*, 093520.
[15] Y. Sun, C. Liu, D. C. Grauer, J. Yano, J. R. Long, P. Yang, C. J. Chang, *J. Am. Chem. Soc.* **2013**, *135*, 17699.
[16] Y. F. Nicolau, M. Dupuy, M. Brunel, *J. Electrochem. Soc.* **1990**, *137*, 2915.
[17] H. M. Pathan, C. D. Lokhande, *Bull. Mater. Sci.* **2004**, *27*, 85.
[18] J. L. Plaza, O. Martínez, S. Rubio, V. Hortelano, E. Diéguez, *CrystEngComm* **2013**, *15*, 2314.
[19] G. Hodes, *Phys. Chem. Chem. Phys.* **2007**, *9*, 2181.
[20] J. Cheng, D. B. Fan, H. Wang, B. W. Liu, Y. C. Zhang, H. Yan, *Semicond. Sci. Technol.* **2003**, *18*, 676.
[21] P. K. Nair, M. T. S. Nair, V. M. García, O. L. Arenas, A. C. Y. Peña, I. T. Ayala, O. Gomezdaza, A. Sánchez, J. Campos, H. Hu, R. Suárez, M. E. Rincón, *Sol. Energy Mater. Sol. Cells* **1998**, *52*, 313.
[22] R. S. Mane, C. D. Lokhande, *Mater. Chem. Phys.* **2000**, *65*, 1.
[23] R. S. Mane, B. R. Sankapal, C. D. Lokhande, *Thin Solid Films* **1999**, *353*, 29.
[24] J. D. Desai, C. D. Lokhande, *Mater. Chem. Phys.* **1993**, *34*, 313.
[25] T. Othani, *J. Phys. Soc. Jpn.* **1974**, *37*, 701.
[26] A. B. F. Martinson, S. C. Riha, E. Thimsen, J. W. Elam, M. J. Pellin, *Energy Environ. Sci.* **2013**, *6*, 1868.
[27] Q. Yang, C. Hu, S. Wang, Y. Xi, K. Zhang, *J. Phys. Chem. C* **2013**, *117*, 5515.
[28] M. Karabulut, H. Ertap, H. Mammadov, G. Ugurlu, M. K. Ozturk, *Turk. J. Phys.* **2014**, *38*, 104.
[29] G. K. Rao, *Mater. Sci. Semicond. Process.* **2014**, *26*, 137.
[30] H. Khallaf, I. O. Oladeji, G. Chai, L. Chow, *Thin Solid Films* **2008**, *516*, 7306.
[31] T. Shibata, Y. Muranushi, T. Miura, T. Kishi, *J. Phys. Chem. Solids* **1991**, *52*, 551.
[32] P. Sinsermsuksakul, J. Heo, W. Noh, A. S. Hock, R. G. Gordon, *Adv. Energy Mater.* **2011**, *1*, 1116.
[33] C. Ulutas, E. Guneri, F. Kirmizigul, G. Altindemir, F. Gode, C. Gumus, *Mater. Chem. Phys.* **2011**, *138*, 817.
[34] R. Bichsel, F. Levy, *J. Phys. D: Appl. Phys.* **1986**, *19*, 1809.
[35] W. Zhao, T. Q. Lin, S. R. Sun, H. Bi, P. Chen, D. Y. Wan, F. Q. Huang, *J. Mater. Chem. A* **2013**, *1*, 194.
[36] B. Cai, Y. Xing, Z. Yang, W.-H. Zhang, J. Qiu, *Energy Environ. Sci.* **2013**, *6*, 1480.
[37] J. H. Heo, S. H. Im, J. H. Noh, T. N. Mandal, C.-S. Lim, J. A. Chang, Y. H. Lee, H.-J. Kim, A. Sarkar, Md. K. Nazeeruddin, M. Gratzel, S. I. Seok, *Nat. Photonics* **2013**, *7*, 486.
[38] W. H. Nguyen, C. D. Bailie, E. L. Unger, M. D. McGehee, *J. Am. Chem. Soc.* **2014**, *136*, 10996.
[39] B. Xu, E. Sheibani, P. Liu, J. Zhang, H. Tian, N. Vlachopoulos, G. Boschloo, L. Kloo, A. Hagfeldt, L. Sun, *Adv. Mater.* **2014**, *26*, 6629.
[40] J. H. Kim, P.-W. Liang, S. T. Williams, N. Cho, C.-C. Chueh, M. S. Glaz, D. S. Ginger, A. K.-Y. Jen, *Adv. Mater.* **2015**, *27*, 695.
[41] A. Yella, H.-W. Lee, H. N. Tsao, C. Yi, A. K. Chandiran, M. K. Nazeeruddin, E. W.-G. Diau, C.-Y. Yeh, S. M. Zakeeruddin, M. Grätzel, *Science* **2011**, *334*, 629.
[42] W. Ke, G. Fang, H. Tao, P. Qin, J. Wang, H. Lei, Q. Liu, X. Zhao, *ACS Appl. Mater. Interfaces* **2014**, *6*, 5525.
[43] S. Yun, A. Hagfeldt, T. Ma, *Adv. Mater.* **2014**, *26*, 6210.
[44] M. X. Wu, X. Lin, T. H. Wang, J. S. Qiu, T. L. Ma, *Energy Environ. Sci.* **2011**, *4*, 2308.
[45] J. D. Roy-Mayhew, D. J. Bozym, C. Punckt, I. A. Aksay, *ACS Nano* **2010**, *4*, 6203.
[46] K. M. Lee, C. Y. Hsu, P. Y. Chen, M. Ikegami, T. Miyasaka, K. C. Ho, *Phys. Chem. Chem. Phys.* **2009**, *11*, 3375.
[47] Q. Tai, B. Chen, F. Guo, S. Xu, H. Hu, B. Sebo, X.-Z. Zhao, *ACS Nano* **2011**, *5*, 3795.
[48] M. K. Wang, A. M. Anghel, B. Marsan, N. C. Ha, N. Pootrakulchote, S. M. Zakeeruddin, M. Gratzel, *J. Am. Chem. Soc.* **2009**, *131*, 15976.
[49] M. Wu, T. Ma, *J. Phys. Chem. C* **2014**, *118*, 16727.
[50] Y. Xiao, G. Han, H. Zhou, Y. Li, J.-Y. Lin, *Electrochim. Acta* **2015**, *155*, 103.
[51] S.-H. Hsu, C.-T. Li, H.-T. Chien, R. R. Salunkhe, N. Suzuki, Y. Yamauchi, K.-C. Ho, K. C.-W. Wu, *Sci. Rep.* **2014**, *4*, 6983.
[52] X. Yang, L. Zhou, A. Feng, H. Tang, H. Zhang, Z. Ding, Y. Ma, M. Wu, S. Jin, *J. Mater. Res.* **2014**, *29*, 935.
[53] H. Chen, L. Zhu, H. Liu, W. Li, *J. Phys. Chem. C* **2013**, *117*, 3739.
[54] S. A Patil, D. V. Shinde, I. Lim, K. Cho, S. S. Bhande, R. S. Mane, N. K. Shrestha, J. K. Lee, T. H. Yoon, S.-H. Han, *J. Mater. Chem. A* **2015**, *3*, 7900.
[55] X. Xin, M. He, W. Han, J. Jung, Z. Lin, *Angew. Chem. Int. Ed.* **2011**, *50*, 11739.
[56] S. Thomas, T. G. Deepak, G. S. Anjusree, T. A. Arun, S. V. Nair, A. S. Nair, *J. Mater. Chem. A* **2014**, *2*, 4474.
[57] F. Gong, H. Wang, X. Xu, G. Zhou, Z.-S. Wang, *J. Am. Chem. Soc.* **2012**, *134*, 10953.

[58] X. Xu, D. Huang, K. Cao, M. Wang, S. M. Zakeeruddin, M. Grätzel, *Sci. Rep.* **2013**, *3*, 1489.
[59] M. Gao, W. Sheng, Z. Zhuang, Q. Fang, S. Gu, J. Jiang, Y. Yan, *J. Am. Chem. Soc.* **2014**, *136*, 7077.
[60] Y. Liang, Y. Li, H. Wang, J. Zhou, J. Wang, T. Regier, H. Dai, *Nat. Mater.* **2011**, *10*, 780.
[61] M.-R. Gao, X. Cao, Q. Gao, Y.-F. Xu, Y.-R. Zheng, J. Jiang, S.-H. Yu, *ACS Nano* **2014**, *8*, 3970.
[62] T. F. Jaramillo, K. P. Jorgensen, J. Bonde, J. H. Nielsen, S. Horch, I. Chorkendorff, *Science* **2007**, *317*, 100.
[63] J. Kibsgaard, Z. Chen, B. N. Reinecke, T. F. Jaramillo, *Nat. Mater.* **2012**, *11*, 963.
[64] Y. G. Li, H. L. Wang, L. M. Xie, Y. Y. Liang, G. S. Hong, H. Dai, *J. Am. Chem. Soc.* **2011**, *133*, 7296.
[65] J. Yang, D. Voiry, S. J. Ahn, D. Kang, A. Y. Kim, M. Chhowalla, H. S. Shin, *Angew. Chem. Int. Ed.* **2013**, *52*, 13751.